Neuron
Article

A Putative Vesicular Transporter Expressed in *Drosophila* Mushroom Bodies that Mediates Sexual Behavior May Define a Neurotransmitter System

Elizabeth S. Brooks,[1] Christina L. Greer,[1] Rafael Romero-Calderón,[1] Christine N. Serway,[1] Anna Grygoruk,[1] Jasmine M. Haimovitz,[1] Bac T. Nguyen,[1] Rod Najibi,[1] Christopher J. Tabone,[2,3] J. Steven de Belle,[2,4] and David E. Krantz[1,*]

[1]Department of Psychiatry and Biobehavioral Sciences, Hatos Center for Neuropharmacology and Jane & Terry Semel Institute for Neuroscience and Human Behavior, The David Geffen School of Medicine at UCLA, Room 3357C, Gonda (Goldschmied) Center for Genetic and Neuroscience Research, 695 Charles Young Drive, Los Angeles, CA 90095-1761, USA
[2]School of Life Sciences, University of Nevada, Las Vegas, 4505 Maryland Parkway, Las Vegas, NV 89154-4004, USA
[3]Present address: Smurfit Institute of Genetics, Trinity College, Dublin, Ireland
[4]Present address: Dart Neuroscience LLC, 7473 Lusk Boulevard, San Diego, CA 92121-5707, USA
*Correspondence: dkrantz@ucla.edu
DOI 10.1016/j.neuron.2011.08.032

SUMMARY

Vesicular transporters are required for the storage of all classical and amino acid neurotransmitters in synaptic vesicles. Some neurons lack known vesicular transporters, suggesting additional neurotransmitter systems remain unidentified. Insect mushroom bodies (MBs) are critical for several behaviors, including learning, but the neurotransmitters released by the intrinsic Kenyon cells (KCs) remain unknown. Likewise, KCs do not express a known vesicular transporter. We report the identification of a novel *Drosophila* gene *portabella* (*prt*) that is structurally similar to known vesicular transporters. Both larval and adult brains express PRT in the KCs of the MBs. Additional PRT cells project to the central complex and optic ganglia. *prt* mutation causes an olfactory learning deficit and an unusual defect in the male's position during copulation that is rescued by expression in KCs. Because *prt* is expressed in neurons that lack other known vesicular transporters or neurotransmitters, it may define a previously unknown neurotransmitter system responsible for sexual behavior and a component of olfactory learning.

INTRODUCTION

Synaptic transmission with classical neurotransmitters depends on two classes of structurally and pharmacologically distinct neurotransmitter transporters. These include (1) vesicular transporters that localize to synaptic vesicles, actively driving transmitter into the vesicular lumen and (2) plasma membrane transporters that terminate neurotransmission by the uptake of neurotransmitter into either the presynaptic site of release or adjacent cells. The number of known vesicular transporters is surprisingly small and includes four distinct families for the transport of the following: (1) monoamines, such as dopamine and serotonin (VMAT1 and VMAT2); (2) GABA and glycine (VGAT or VIAAT); (3) acetylcholine (VAChT); and (4) glutamate (VGLUT1-3; Chaudhry et al., 2008). Additional transporters for purine nucleotides (Sawada et al., 2008) and aspartate (Miyaji et al., 2008) have recently been identified as part of the SLC17 family, related to VGLUTs. Any other novel neurotransmitters used by invertebrates and/or mammals would similarly require a distinct vesicular transporter for storage and exocytotic release.

In *Drosophila* and other insects, the mushroom bodies (MBs) play a critical role in olfactory learning, as well as integrating information from other sensory modalities (Davis, 2011; Keene and Waddell, 2007; Strausfeld et al., 1998; Wessnitzer and Webb, 2006). Kenyon cells (KCs) form all of the intrinsic fiber tracts of the MBs, whereas several extrinsic neurons project into the MBs, providing input and output of information and/or regulating KC function (Tanaka et al., 2008). To date, neither the neurotransmitter released from the intrinsic neurons nor the vesicular transporter responsible for its storage has been identified. Of the known neurotransmitter systems, the vesicular transporters for amines (DVMAT), GABA (DVGAT), and glutamate (DVGLUT) are absent from KCs (Chang et al., 2006; Daniels et al., 2008; Fei et al., 2010). Although expression data for the vesicular acetylcholine transporter is not available, the biosynthetic enzyme responsible for Ach synthesis is also absent from KCs (Gorczyca and Hall, 1987; Yasuyama et al., 2002). Several classical and peptide neurotransmitters have been identified in processes that project into the MBs (Davis, 2011). In contrast, although multiple candidates have been suggested (Schäfer et al., 1988; Schürmann, 2000; Sinakevitch et al., 2001), the neurotransmitter released from the KCs is not known and could possibly constitute a previously undescribed neurotransmitter system.

The MBs have been implicated in other behaviors, including sleep (Joiner et al., 2006), aggression (Baier et al., 2002), and motor activity (Serway et al., 2009). Furthermore, both the MBs

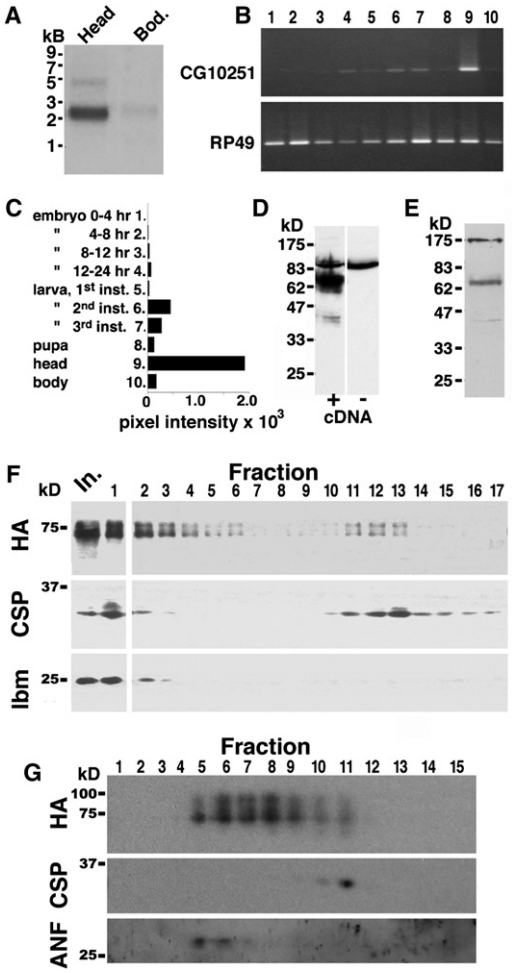

Figure 1. Expression of *CG10251* mRNA, Protein, and Subcellular Localization

(A) Northern blots show expression of *CG10251* mRNA in heads and, to a lesser extent, in bodies.

(B) PCR using a panel of cDNAs from various developmental stages (see labels in panel C) confirmed high expression of *CG10251/prt* in adult heads, relative to the body, as well as some expression in larva, and minimal expression during pupal and embryonic stages (top). Identical samples were amplified with a probe to the widely expressed gene *RP49* (bottom).

(C) Normalized levels of *CG10251* expression are shown graphically.

(D and E) Expression of the CG10251 protein.

(D) Homogenates from wild-type S2 cells (−) and cells expressing the *CG10251/prt* cDNA (+) were probed on western blots using the CG10251 antiserum. We detected a band at ~70 kDa in cells expressing CG10251, but not in wild-type cells.

(E) Homogenates from wild-type adult heads showed a similarly migrating band at ~70 kDa.

(F and G) CG10251/PRT protein localizes to both SV and dense fractions.

(F) Homogenates from flies expressing a HA-tagged version of PRT were fractionated on a linear glycerol velocity gradient followed by western blotting with primary antibodies to HA (top), cysteine string protein (CSP, a marker for SVs, middle panel), and late bloomer (lbm, a marker for the plasma membrane, bottom). For all three antibodies, the input lane (In.) and cushion (fraction 1) were processed separately to prevent overexposure, allowing better visualization of the relevant bands.

(G) Homogenates from flies expressing a HA-tagged version of PRT were fractionated on a linear sucrose density gradient followed by western blotting with primary antibodies to HA (top), CSP (middle), and the fusion protein containing atrial natriuretic factor (ANF) and GFP (bottom, a marker for LDCVs). Molecular weight markers (kDa) are shown on the left side of the figure.

and the central complex (CCX) have been linked to aspects of sexual behavior (O'Dell et al., 1995; Popov et al., 2003; Sakai and Kitamoto, 2006). Sexual behavior has been studied extensively in the fly, with a particular focus on courtship, although a handful of mutations affecting copulation have been described (Yamamoto et al., 1997). The neurocircuitry underlying all of these behaviors remains poorly understood.

We report here the molecular cloning of a novel, putative vesicular transporter (*CG10251*) that localizes to the MBs and processes that innervate the CCX. Mutation of *CG10251* inhibits learning and causes a dramatic sexual phenotype in which the male fly is unable to correctly position himself during copulation. The copulation deficit was rescued by expression of CG10251 in the MBs, suggesting a previously unknown function for this structure. We speculate that the CG10251 protein may be responsible for the storage of a previously unknown type of neurotransmitter in a subset of KCs and several other neurons in the insect nervous system. We have named the *CG10251* gene *portabella* (*prt*).

RESULTS

Identification of a Novel Gene Similar to Both Vesicular Monoamine and Acetylcholine Transporters

The *D. melanogaster* genome contains orthologs of all known vesicular neurotransmitter transporters, including genes similar to *VGLUT*, *VMAT*, *VAChT*, and *VGAT* (Daniels et al., 2004; Fei et al., 2010; Greer et al., 2005; Kitamoto et al., 1998). We searched the genomic database for genes similar to *Drosophila VMAT* (*DVMAT*) to identify additional, potentially novel vesicular transporters. We identified a gene similar to both *DVMAT* and *DVAChT* that localizes to cytogenetic region 95A on chromosomal arm 3R. *DVMAT* and *DVAChT* localize to cytogenetic regions 50B (2R) and 91C (3R), respectively. We found that CG10251 shows 35.8% similarity to DVMAT and 30.2% similarity to DVAChT (see Figure S1 available online). In comparison, DVMAT and DVAChT share 35.5% similarity. The long open reading frame of CG10251 contains 12 predicted transmembrane domains similar to both mammalian and *Drosophila* VMAT and VAChT.

RNA and Protein Expression

To confirm that *CG10251* RNA is expressed in vivo, we probed northern blots of adult fly heads and bodies (Figure 1A). We detected a major band migrating at just above the 2 kb marker and a minor species at 5 kb. We also detected the ~2 kb species in bodies but at low levels relative to heads. We observed similar enrichment in heads for *DVMAT* and other neurotransmitter transporters (Greer et al., 2005; Romero-Calderón et al., 2007). The size of the major *CG10251* mRNA species was similar to the cDNA we obtained with RT-PCR (2.2 kb), suggesting that we identified the full extent of the major *CG10251* transcript. Repeated trials of 5′ and 3′ rapid amplification of cDNA ends did not reveal additional exons (data not shown); thus, the minor

5 kb species likely represents an mRNA precursor, although we cannot rule out the possibility of a low-abundance splice variant.

We performed PCR with a commercially available cDNA panel representing various developmental stages and a *CG10251*-specific primer set (Figures 1B and 1C). Our data suggest that *CG10251* is primarily expressed during adulthood and late larval stages rather than during embryonic development. We have attempted in situ hybridization of embryos for *CG10251* expression, but have been unable to detect a signal (data not shown), possibly due to the low levels of *CG10251* mRNA at this stage.

We next generated an antibody against the CG10251 carboxyl terminus and probed homogenates of S2 cells transfected with *CG10251* cDNA to test its activity (Figure 1D). Cells expressing CG10251 (+) showed a broad 70 kDa signal, whereas untransfected S2 cells (−) did not. We probed homogenates of adult heads and detected a band at 70 kDa, as well as additional bands at the top of the gel that may represent nonspecific cross-reactivity (Figure 1E). A faint band immediately above the major band suggests that a portion of CG10251 may undergo posttranslational modification. This species was more visible in biochemically fractionated samples (see below). Another faint band at 40 kDa may represent a degradation product. We confirmed the specificity of the antiserum with the *CG10251* mutant (see below). We thus demonstrated the in vivo expression of both *CG10251* mRNA and protein.

Biochemical Fractionation

The similarity of *CG10251* to *DVMAT* and *DVAChT* suggests that it, too, might encode a vesicular transporter. CG10251 localized to intracellular membranes at steady state when expressed in S2 cells, and in vitro endocytosis assays revealed that CG10251 internalized from the cell surface, as we have observed for DVMAT and DVGLUT (data not shown). We therefore tested whether the protein would also localize to synaptic vesicles (SVs) in vivo. Relatively low expression of endogenous CG10251 made it difficult to detect in initial biochemical fractionation experiments (data not shown). To facilitate these analyses, we created a fly transgene expressing a hemagglutinin (HA)-tagged version of the protein and used the panneuronal *elav-Gal4* driver. To determine whether CG10251 localizes to SVs, we applied homogenates from flies expressing CG10251 to a glycerol velocity gradient. A portion of CG10251 peaked in fractions containing the peak for SV marker cysteine string protein (CSP; fractions 11–13; Figure 1F). These data suggest that at least a fraction of the protein localizes to SVs, consistent with the prediction from sequence analysis that CG10251 is a vesicular transporter.

We also performed sucrose density fractionation to determine whether CG10251 might localize to other types of secretory vesicles, in particular large dense core vesicles (LDCVs). We found that whereas some CG10251 colocalized with CSP in light fractions, most of the immunoreactivity was found in heavier fractions, some coincident with a fusion protein containing mammalian atrial natriuretic factor (ANF; Figure 1G), a marker for LDCVs (Rao et al., 2001). These data suggest that CG10251 likely localizes to LDCVs as well as SVs, similar to mammalian VMAT2, which preferentially localizes to LDCVs in cultured cells and in vivo (Nirenberg et al., 1995).

Localization in the Larval Nervous System

To localize CG10251 in vivo, we labeled whole mounts of third-instar larval brain and ventral ganglia. A small subset of cells in the ventral ganglia expressed CG10251 (Figures 2A and 2N). We did not detect significant colocalization with 5-HT, TH, or Ddc (data not shown). Thus, CG10251 is unlikely to store either dopamine or serotonin, in contrast to DVMAT, which localizes to these cell types (Greer et al., 2005). Other aminergic transmitters in the fly include octopamine and tyramine; however, DVMAT is likely responsible for their transport as well (Greer et al., 2005), and both localize to large midline cells (Monastirioti et al., 1995; Nagaya et al., 2002). We did not detect cells expressing CG10251 at the midline.

In the larval brain, we observed robust expression of CG10251 in the MBs (Figures 2D–2M). To confirm localization to cells in the MBs, we expressed *mCD8-GFP* with the MB driver *0K107-Gal4* (Figures 2E and 2H; Connolly et al., 1996) and colabeled larval brains for CG10251 (Figures 2D and 2G). We observed overlap in the cell bodies of the KCs, their dendrites, which make up the calyces, and their axons, which comprise the medial and vertical lobes of the MBs (Figures 2D–2I). These data indicate that CG10251 is expressed by at least a subset of the KCs intrinsic to the MBs and therefore may be responsible for storage of neurotransmitter in these cells. In light of this expression pattern and the proposed transport function of CG10251, we have renamed the gene *portabella* (*prt*) and refer to the CG10251 protein as PRT.

We note that subsets of KCs did not appear to be labeled (asterisks, Figure 2K) by the PRT antibody. A similar pattern has been reported for several developmental markers expressed in KCs (Noveen et al., 2000), suggesting that PRT may be expressed at a relatively late stage during differentiation and perhaps only in a subpopulation of KCs.

We observed PRT expression in at least one bilateral extrinsic neuron projecting ipsilaterally to the vertical and medial lobes of the larval MBs (arrowheads, Figures 2L and 2M). The location of and projections from this cell appear similar to that described for a neuron expressing the amnesiac peptide, which is critical for memory formation in *Drosophila* (Waddell et al., 2000). However, colabeling experiments suggest that the extrinsic neurons expressing PRT are distinct from those expressing the amnesiac peptide (Figure S2). Expression of PRT in these cells and four other small clusters in the larval brain is shown schematically in Figure 2N.

Localization in the Adult Nervous System

The *Drosophila* nervous system undergoes extensive remodeling during metamorphosis, resulting in adult MBs that are morphologically distinct from the larval structures. In the adult, each vertical lobe of the MB can be recognized as distinct α and α' lobes, and the medial lobes include distinct β, β', and γ lobes (Crittenden et al., 1998). We observed strong PRT expression in the adult MBs, including labeling of all five lobes (Figures 3A–3C). Relative to the lobes, labeling of the calyx and KC bodies was less intense in the adult than in the larva (Figure 3E). This pattern likely reflects the localization of the protein to secretory vesicles that are concentrated in the axons and are less abundant in mature dendrites and cell bodies.

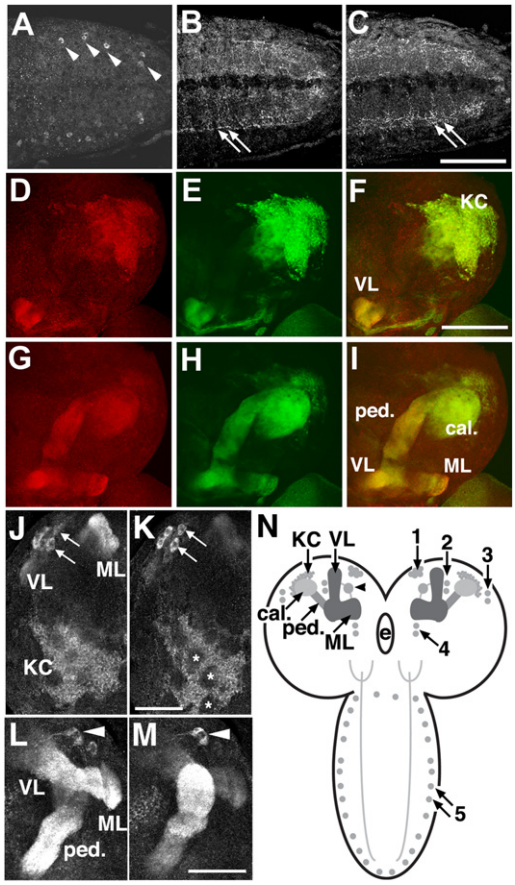

Figure 2. Localization of PRT in the Larval Ventral Ganglion

(A–C) One to two cell bodies per hemisegment express PRT and localize to lateral aspects of the ventral nerve cord. Processes project medially into the neuropil in a complex pattern that runs throughout the ventral ganglion. Confocal images show selected optical slices though the caudal aspect of the ventral ganglion to show the labeled cell bodies (A, arrowheads) and neuropil (B and C, arrows). Scale bar represents 50 μm.

(D–I) PRT expression in larval mushroom bodies. Larval brains expressing a membrane-bound form of GFP (*mCD8-GFP*) with the MB driver *OK107-Gal4* were labeled for PRT, followed by a Cy3-conjugated secondary antibody. Confocal images show a dorsalateral view of the brain (D–F) and more ventromedial sections (G–I). GFP expression (green), PRT labeling (red) and the merged images (F and I) are shown as horizontal sections with dorsal-posterior regions at the top of each image. We detect PRT in all aspects of the MBs, including the Kenyon cells (KC), calyx (cal), the penduncle (ped), and the vertical and medial lobes (VL and ML). Scale bar represents 100 μm.

(J–M) Expression in larval Kenyon cells, a ventromedial cluster of cells, and a large extrinsic neuron. Panels show horizontal sections with the posterior side down. Scale bars represent 50 μm. See also Figure S2.

(J and K) Two optical sections show expression of PRT in the KC of the larval MBs. Patches of unlabeled areas in the center of the KC cluster are indicated (K, asterisks). A small portion of the ML and VL are visible in (J). An additional group of four to five cells (arrows) at the ventral-medial aspect of each vertical lobe are also labeled.

(L and M) Two optical sections show a large extrinsic neuron (arrowhead) sending processes to both the ML and VL. The peduncle of the MB is also indicated (ped).

(N) In the frontal perspective cartoon, the KC bodies are shown as light gray circles. Processes from these cells project ventrally and rostrally to form the peduncle (ped), then branch into medial and vertically projecting lobes in the central brain. The dendrites of the KCs form the calyx (cal). A relatively large, bilaterally symmetric extrinsic neuron expressing PRT projects into each ipsilateral MB. Additional cells expressing PRT in the brain and ventral ganglia are indicated as darker gray circles, and prominently labeled processes are indicated with stippling. The numbers represent arbitrary designations of cell clusters in the larva. e indicates esophageal foramen.

We also detected PRT expression in the peduncle, formed by KC axons before they branch into the lobes (Figures 3D–3F). PRT was not distributed uniformly throughout the peduncle, and a portion of the core was weakly labeled (Figures 3D–3F; data not shown). This pattern suggests that PRT may not be expressed in all KCs, although further experiments will be needed to confirm this. Several additional cell bodies near the MBs express PRT (Figures 3A–3C and 3F), as well as one cluster of two to three cells in the subesophageal ganglion that projects medially toward the esophogeal foramen (arrows, Figure 3F).

During metamorphosis there is also extensive development of the central complex, a midline structure just posterior to the MB medial lobes involved in motor activity (Strauss, 2002) and visual memory (Liu et al., 2006). PRT labeling of the adult brain revealed that it is expressed in components of the CCX, including the neuropil of the ellipsoid and fan-shaped bodies (Figures 3G and 3H).

We also detected PRT expression in two bilaterally symmetric clusters of two and three cells, each near the medial aspect of the optic lobe, that project outward toward the medulla (asterisks, Figure 3I). The cartoon in Figure 3J summarizes the PRT expressing cells in the adult. Other than the KCs, there are approximately 56 labeled cell bodies. For comparison, the adult brain contains approximately 300 dopaminergic and 106 serotonergic cells (Monastirioti, 1999).

To complete our survey of the adult central nervous system, we also labeled the thoracic ganglion and found three clusters with two to four cells each that lie near the ventral midline (Figures 3K–3M). This expression pattern was not sexually dimorphic (Figures 3L and 3M).

Generation of a *prt* Mutant

To investigate the function of PRT, we generated a mutant fly. A survey of the public database revealed a previously generated line with a *SUPor-P* element inserted into the 5′ untranslated region (UTR) of *prt* (Figure 4A). Line KG07780 was obtained from the Bloomington Stock Center (Indiana University), and we confirmed that the *SUPor-P* element was located 118 bp upstream of the predicted initiating methionine (data not shown). We used imprecise excision to generate a *prt* mutation. Lines were screened by PCR, with primers flanking the *P* element insertion. In wild-type Canton-S (CS) flies, we detected a major product that migrated at 1.2 kb, consistent with the size predicted by the primary sequence (Figure 4B). In one line, the major band migrated at 400 bp, consistent with an 850 bp deletion (Figure 4B). We designated this allele prt^1. We immunolabeled adult brains to determine whether prt^1 mutants produce any residual protein, and we failed to detect any labeling of the MBs or elsewhere (Figure 4C). These data confirm the specificity of the antiserum to PRT. In addition, the size of the deletion and the absence of residual protein suggest that prt^1 is either a severe hypomorph or a null mutation (see also deficiency analysis below).

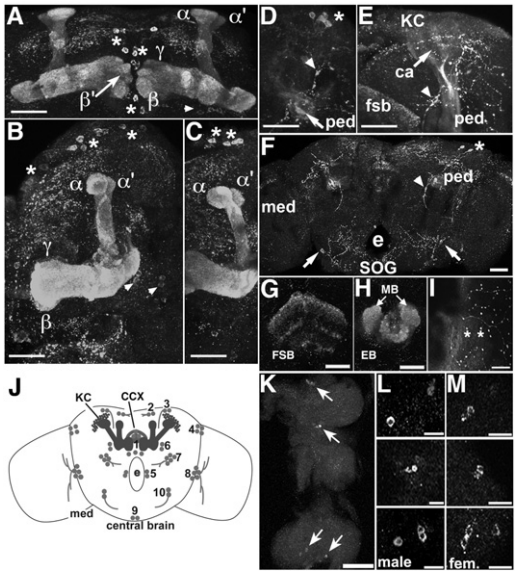

Figure 3. PRT Expression in Adult Mushroom Bodies, Central Complex, and Thoracic Ganglion

(A–F) PRT is expressed in the medial lobes β, γ (A and B), β' (A), ped (D–F), and the vertical lobes α and α' (A–C). Additional labeled cell bodies are indicated with asterisks (A–D and F), arrowheads (A and B), and arrows (F). Arrowheads also indicate labeled projections (D–F). Scale bars represent 25 μm. e indicates esophageal foramen and SOG indicates subesophageal ganglion.

(D–F) Optical sections through the peduncle show expression in a subset of fibers on the lateral edge and in the center. Labeling of the KCs and calyx (E) is low intensity relative to the lobes, consistent with our expectation that a vesicular transporter would localize primarily to the axons and terminals of a mature neuron, rather than the cell bodies and dendrites.

(G–I) Projections to the central complex and medulla in the adult brain. PRT is expressed in both the fan-shaped body (G; FSB) and the ellipsoid body (H; EB) of the central complex. Additional labeling (H) represents the tips of the MB medial lobes. Cell bodies at the border between the central brain and the medulla arborize in the medulla and show prominent varicosities (I, asterisks). Scale bars represent 25 μm in (G) and (H) and 10 μm in (I).

(J) The schematic shows a frontal view of the central brain that summarizes expression of PRT in the adult, including expression in the MBs and the central complex, shown in solid gray. Additional neurons and processes expressing PRT are shown as gray circles or stippling, respectively. The numbers represent arbitrary designations of cell clusters in the adult.

(K) Arrows indicate clusters of two to four labeled cell bodies in the thoracic ganglion. Anterior is up, posterior down. Scale bar represents 50 μm.

(L and M) Higher magnification of the three cell clusters with the anterior cluster at the top, posterior cluster at the bottom, showing no sexual dimorphism between the male (L) and female (M). Scale bars represent 10 μm.

For both mammals and invertebrates, developmental perturbations of neurotransmitter metabolism can have neuroanatomical sequelae (Budnik et al., 1989; Lawal et al., 2010; Levitt et al., 1997). We therefore analyzed the morphology of the MBs and CCX in the *prt*^{1} mutant and found it grossly intact in paraffin sections of adult brains stained with hematoxylin and eosin staining (H&E; Figure 4D; data not shown). To rule out more subtle neuroanatomical changes, we performed volumetric analyses of the MB calyx and CCX (ellipsoid body + fan-shaped body). We detected no difference in either calyx or CCX volume between CS and *prt*^{1} (Figures 4E and 4F), indicating that *prt*^{1} does not result in significant anatomical defects.

Behavioral Analysis

To further examine changes in the function of the MBs and other tissues expressing PRT, we investigated *prt*^{1} mutant behavior. We first outcrossed the *prt*^{1} flies for six generations into the wild-type strain CS. Outcrossing removed a closely linked mutation that reduced viability and fertility (data not shown), and all behavioral experiments were performed using the outcrossed lines. The outcrossed *prt*^{1} flies were viable, fertile, and showed no obvious external morphological defects.

The relatively high level of PRT expression in the MBs, as compared to other structures, suggests that it may play a role in olfactory classical conditioning, which is known to require the MBs (Davis, 2011). We used a modified T maze to test olfactory classical conditioning, as previously described (de Belle and Heisenberg, 1994). As controls for these experiments, we first established that *prt*^{1} flies had normal avoidance of both electric shock and the odors used to test learning (Figures 5A–5C). We next tested olfactory learning. We found that *prt*^{1} mutants have a learning defect, evidenced by a decreased performance index immediately following training (Figure 5D). The performance indices for *prt*^{1} were also reduced at 30 min and 6 hr after training (Figure 5D). The difference between CS and *prt*^{1} was consistent over short-term (30 min) and middle-term (6 hr) phases of memory, suggesting normal memory decay in *prt*^{1} flies.

We next tested *prt*^{1} behavior using several other well-established assays. Performance indices for negative geotaxis and fast phototaxis were equivalent to those of wild-type flies (Figures S3A and S3B), indicating that gross locomotor activity and the response to both mechanical stimuli and visible light are intact in *prt*^{1}. We did find a modest impairment in courtship behavior. Although *prt*^{1} males performed all of the necessary courting rituals, they spent less time courting (Figure 6A).

In the course of performing courtship assays, copulation was observed. Normally, males mount the female from behind, curling their abdomen upwards to allow coupling. Once coupled, the male maintains a forward-facing orientation in the same direction as the female (Figure 6B, top pictures; Movie S1). Copulation typically lasts ~20 min (Jagadeeshan and Singh, 2006). For the first several minutes of this period, wild-type pairs may move forward or adjust positions, but for the remainder of this time the flies remain essentially motionless.

Copulation in *prt*^{1} mutants differs dramatically. Similar to wild-type flies, *prt*^{1} males mount the female and curl their abdomen to begin copulation. However, after coupling, the *prt*^{1} male continuously struggles to maintain his orientation and can be seen in a variety of different positions relative to the female (Figure 6B, bottom pictures; Movie S2). We quantified the amount of time that *prt*^{1} males spent in a position distinct from that usually seen in wild-type flies as a percentage of the total copulation duration (Figure 6C). Whereas CS flies primarily remain centered on the dorsal abdomen of the female, *prt*^{1} flies spent nearly half of copulation severely misaligned. Although the genitalia of the male and female remain in contact, the male can be positioned perpendicular to the normal axis or rotated nearly 180° from horizontal. Moreover, during copulation, *prt*^{1} mating pairs move about the observation chamber, with the female dragging the male behind. In cross-genotype mating experiments, *prt*^{1} males mated to CS females showed defective copulation, whereas CS

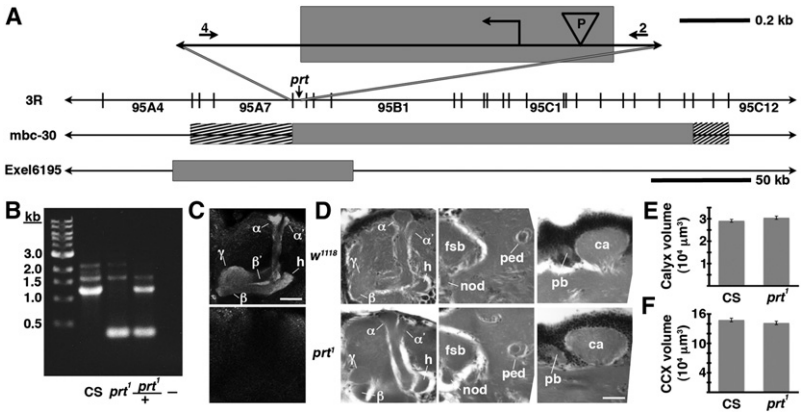

Figure 4. The *prt*^{1} Mutation

(A) The relative position of the *prt* gene is shown in cytological region 95A8 on the third chromosome. The shaded box at the top of the figure represents an approximately 850 bp deletion created with imprecise excision of a *P* element ("P" in the inverted triangle), including the initiating methionine (angled arrow). The numbers 4 and 2 indicate primers used to detect the deletion. The lines below show deficiencies that uncover *prt* (*Df(3R)mbc-30, Df(3R)Exel6195*). The shaded boxes represent the deletion. The cross-hatched boxes indicate breakpoints approximated by polytene chromosome squash. Scale bars represent 50 kb for deficiencies and 0.2 kb for inset.

(B) PCR was used to detect the *prt*^{1} mutation. Wild-type CS flies show a major band at 1.2 kb, *prt*^{1} flies show a major band at 400 bp, and *prt*^{1}/+ heterozygotes show both. – indicates a nontemplate control. A 1 kb standard is shown on the left.

(C) Single confocal slices through the mushroom body lobes of whole-mount brains labeled with anti-PRT. A *w*^{1118} brain is on top with labeling of the MB lobes (α, α', β, β', and γ) and heel (h), and a *prt*^{1} brain is on bottom, showing no detectable anti-PRT labeling. Scale bar represents 20 μm.

(D) H&E-stained paraffin sections show that *prt*^{1} mutants have grossly intact MB morphology (α, α', β, and γ lobes and h, ped, and ca) and central complex (fan-shaped body [fsb], noduli [nod], and protocerebral bridge [pb]). The β' lobe is also grossly intact in *prt*^{1} (not shown). Scale bar represents 20 μm.

(E and F) Volumetric analyses of the MB calyx (E) and CCX (F) in CS and *prt*^{1} did not significantly differ; Student's t test; p = 0.1934 (E) and p = 0.2496 (F). Bars represent mean ± SEM; n = 10 for all groups.

males mated to *prt*^{1} females did not (Figure 6C). Thus, the *prt*^{1} males were primarily, if not exclusively, responsible for the defect in copulation.

To determine whether the change in the males' position was due to a defect in genital morphology, we examined both the *prt*^{1} male and female genitalia using scanning electron microscopy. We found that the external genitalia of *prt*^{1} males and females were indistinguishable from wild-type (Figures S3D and S3E). We also examined the *prt*^{1} males' sex combs, specialized foreleg structures used to grasp the female during copulation (Ahuja and Singh, 2008; Ng and Kopp, 2008). The morphology of *prt*^{1} sex combs was intact in scanning electron micrographs (Figure S3F), without obvious gaps between bristles, although the number of bristles in the *prt*^{1} sex combs was slightly lower than controls (Figure S3G; Ahuja and Singh, 2008; Tokunaga, 1961).

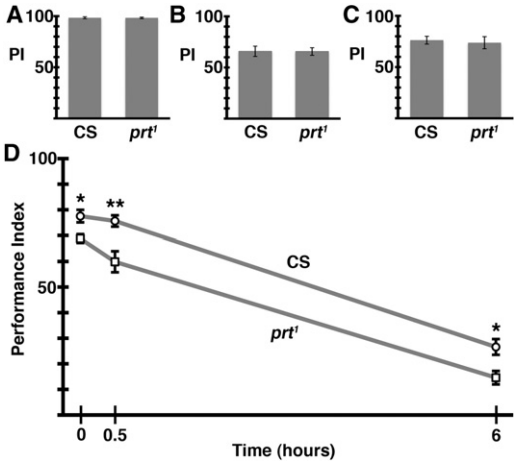

Figure 5. *prt*^{1} Mutants Show a Learning Deficit

(A–C) *prt*^{1} mutants show normal avoidance of electric shock (A) and the odor concentrations used for olfactory learning assays, octanol (10^{-4}) (B), and benzaldhyde (2×10^{-4}) (C). Bars represent mean ± SEM; n = 5 for CS in (A) and n = 6 for all other groups.

(D) Performance indices indicate a learning defect for *prt*^{1}, seen immediately following training (0), decreased short-term memory (0.5), and reduced middle-term memory (6). *p < 0.05 and **p < 0.01.

Statistical analyses included Student's t test for (A)–(C) and two-way analysis of variance (ANOVA) with Bonferroni's post test for (D). Two-way ANOVA reveals no significant interaction of time and genotype (p = 0.3976) suggesting normal memory decay in *prt*^{1}. Symbols represent mean ± SEM; n = 12 for time 0; n = 6 for 0.5 and 6 hours.

We employed deficiency analysis to help determine the severity of the *prt*^{1} sexual phenotype (Figure 6D). Two deficiency lines that uncover the *prt* locus were used, and the extent of their chromosomal deletions is represented in Figure 4A. The copulatory phenotype seen in the *prt*^{1} homozygote was replicated in both the *prt*^{1}/*Df(3R)mbc-30* and *prt*^{1}/*Df(3R)Exel6195* transheterozygotes (Figure 6D). It is possible that the *prt*^{1} copulation phenotype cannot get measurably worse, and further deficiency analysis using other aspects of the *prt*^{1} phenotype will be necessary to more precisely assess the severity of the *prt*^{1} allele. However, in light of our current data showing that the severity of the phenotype seen in *prt*^{1}/*Df* was equivalent to that of the *prt*^{1} homozygotes and of our molecular analysis showing undetectable levels of PRT protein, we conclude that the *prt*^{1} allele is either a severe hypomorph or a null mutation.

prt^{1} mutants were surprisingly fecund given their contorted mating positions. They were able to produce approximately half the number of offspring as CS flies (Figures 6E). Either insemination occurred during periods when the male was correctly oriented, or wild-type position is not required for insemination. The total duration of copulation was also decreased in *prt*^{1} (Figure 7B). It is perhaps surprising that the decrease in copulation time and fecundity were not more severe given the tremendous struggling observed in mating pairs.

Rescue of *prt*^{1} Copulation Phenotype

To confirm that the copulation defects we observed were due to *prt*^{1} rather than another spurious mutation, we performed

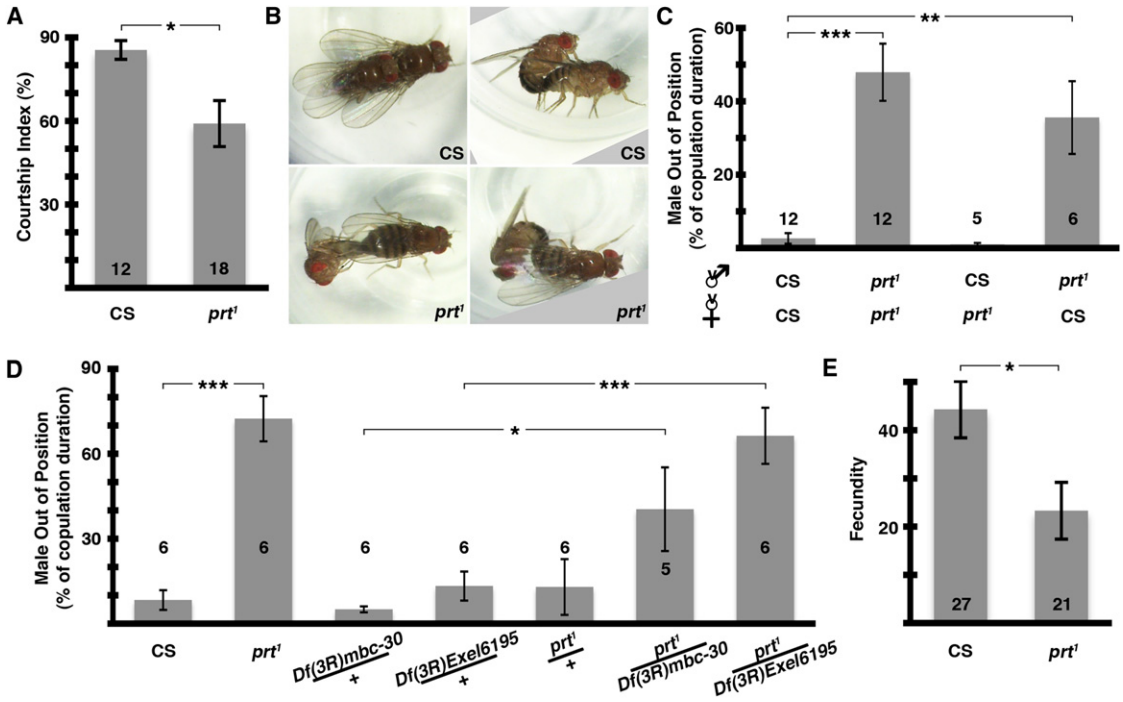

Figure 6. *prt*^{1} Reproductive Behavior

(A) *prt*^{1} mutant males spent 26% less time courting (*p = 0.0182).

(B) The top two panels show normal copulatory positions seen in wild-type flies, and the bottom two panels show improper positioning exemplary of *prt*^{1}.

(C) *prt*^{1} mutants struggle throughout copulation. Quantification of the time a male spends out of position during copulation revealed a significant difference between CS and *prt*^{1} (first two bars, p < 0.001). Intergenotype pairings suggest the *prt*^{1} male was responsible for this phenotype (last two bars, p < 0.01).

(D) Two different deficiencies uncovered *prt*. Both *prt*^{1}/*Df(3R)mbc-30* and *prt*^{1}/*Df(3R)Exel6195* phenocopied the copulation behavior seen in *prt*^{1} (last two columns, p < 0.05 and p < 0.001, respectively).

(E) *prt*^{1} mutants had reduced fecundity (number of progeny/mating pair), 53% that of CS (*p = 0.0167). *p < 0.05, **p < 0.01, and ***p < 0.001.

Statistical analyses included Student's t test for (A) and (E) and ANOVA with Bonferroni's post test for multiple comparisons for all other assays. The data plotted represents mean ± SEM. The n for each group is shown with each column. See also Movies S1 and S2 and Figure S3.

genetic rescue experiments with *UAS-prt* transgenes. The circuitry involved in copulation is not known. Therefore, to maximize our chances of expressing *prt*^{1} in the relevant tissue, we used the broadly distributed driver *daughterless-Gal4* (*Da-Gal4*). As controls, we tested the *Da-Gal4* driver alone and the *UAS-prt* transgenes alone, and none rescued the copulation deficit (Figure 7A). In contrast, when *Da-Gal4* was used in combination with a *UAS-prt* transgene on the third chromosome, we saw rescue of the copulation phenotype (Figure 7A). We replicated these results using a *UAS-prt* transgene on the second chromosome (Figure 7A).

Similarly, we found that the decrease in copulation duration was rescued using *Da-Gal4* and either of these *UAS-prt* transgenes, but not by *Da-Gal4* or *UAS-prt* alone (Figure 7B). Taken together, these data confirm that *prt* plays a critical role in an important but poorly described aspect of *D. melanogaster* sexual behavior.

Although the MBs have been previously linked to courtship behavior (O'Dell et al., 1995; Sakai and Kitamoto, 2006), we wanted to explore whether the MBs could also be involved in copulatory behavior. To this end, we performed genetic rescue experiments using *OK107-Gal4*, a driver commonly used for expression in the MBs (e.g., Connolly et al., 1996). *OK107-Gal4* combined with a *UAS-prt* transgene on either the second or third chromosome resulted in rescue of the copulation phenotype, whereas the controls did not (Figure 7C).

We found that the decrease in copulation duration was also rescued using *OK107-Gal4* and either of these *UAS-prt* transgenes (Figure 7D); the second chromosome *UAS-prt* transgene alone also appeared to rescue copulation duration, presumably due to leaky expression of PRT. Although we cannot rule out the possibility that other cells expressing *OK107-Gal4* are responsible for these effects, these data suggest that the MBs play a critical role in copulatory behavior.

At present, we do not know the PRT substrate, and we suggest that it may be an unknown neurotransmitter. The absence of candidates prevents the validation of PRT's proposed transport activity using most standard biochemical assays. We therefore employed a genetic approach to test the hypothesis that PRT might function as a vesicular transporter in vivo. For mammalian VMATs and VAChT, a wealth of data has identified specific residues required for either transport activity or substrate recognition (see Parsons, 2000 for review; see also Figure S1). A number of these important residues are conserved in DVMAT, DVAChT, and PRT. These include aspartates (D) in the first and tenth transmembrane domains (TM1 and TM10) of DVMAT, DVAChT, and

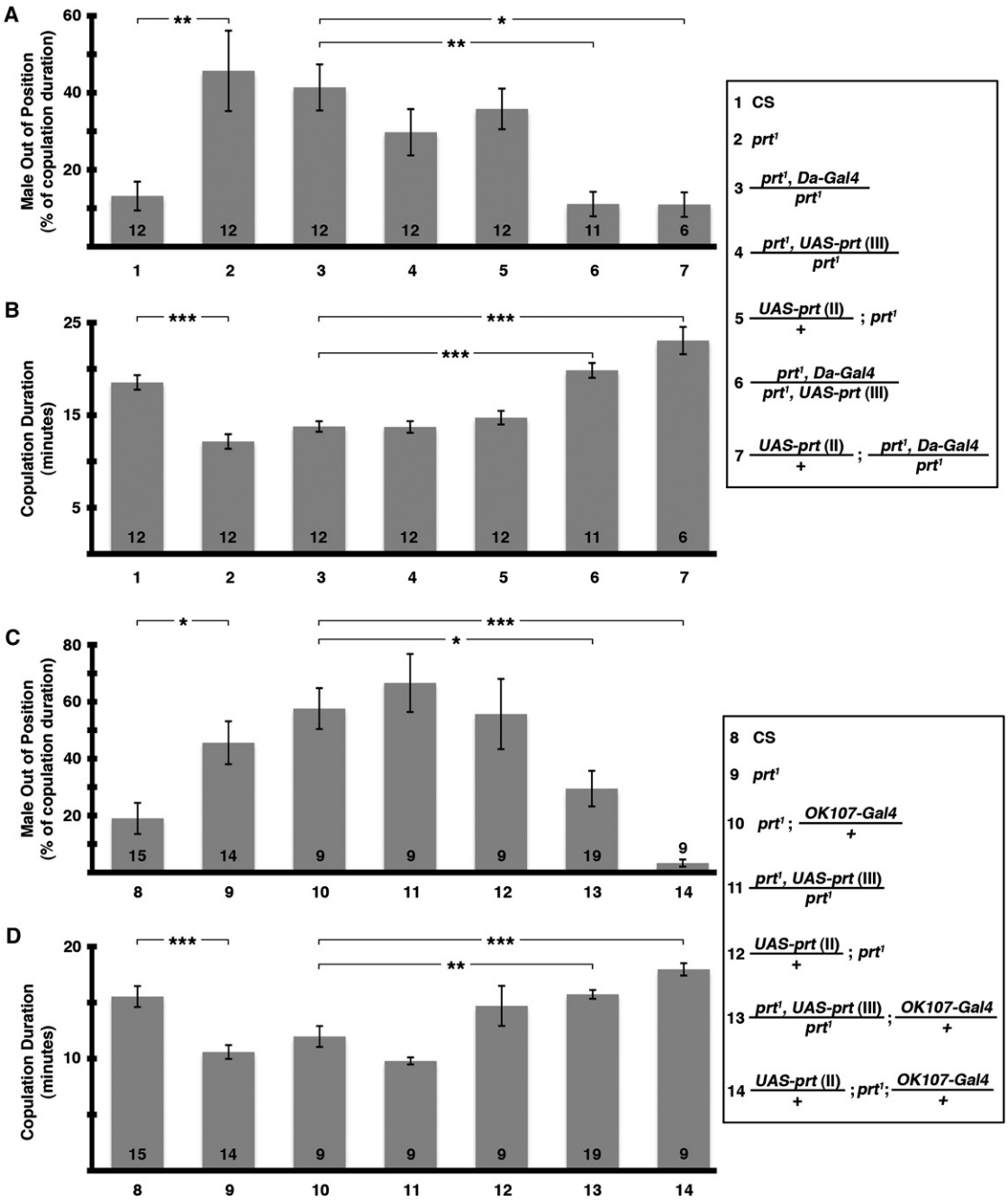

Figure 7. Genetic Rescue of Copulation Defect

(A) The combination of the *Da-Gal4* driver with a *UAS-prt* transgene rescued the copulation phenotype (columns 6 and 7, $p < 0.01$ and $p < 0.05$, respectively); driver or *UAS-prt* transgene alone did not (columns 3–5).

(B) prt^1 mutants had significantly shorter copulation duration than CS (compare columns 1 and 2, $p < 0.001$), rescued with *Da-Gal4* plus *UAS-prt* transgenes (columns 6 and 7, $p < 0.001$ for both), but not driver or *UAS-prt* alone (columns 3–5).

(C) PRT transgenic expression with an MB driver (*OK107-Gal4*) rescued the prt^1 copulation phenotype (columns 13 and 14, $p < 0.05$ and $p < 0.001$, respectively); driver or *UAS-prt* transgenes alone did not (columns 10–12).

(D) The short-duration phenotype was similarly rescued using *OK107-Gal4* plus *UAS-prt* transgenes (columns 13 and 14, $p < 0.01$ and $p < 0.001$, respectively). The *UAS-prt* transgene on the second rescued in the absence of driver, presumably due to leaky PRT expression (column 12, $p < 0.05$ compared to prt^1). See legends on right for genotypes. *$p < 0.05$, **$p < 0.01$, ***$p < 0.001$, ANOVA with Bonferroni's posttest for multiple comparisons. The data plotted represents mean ± SEM. The n for each group is shown with each column.

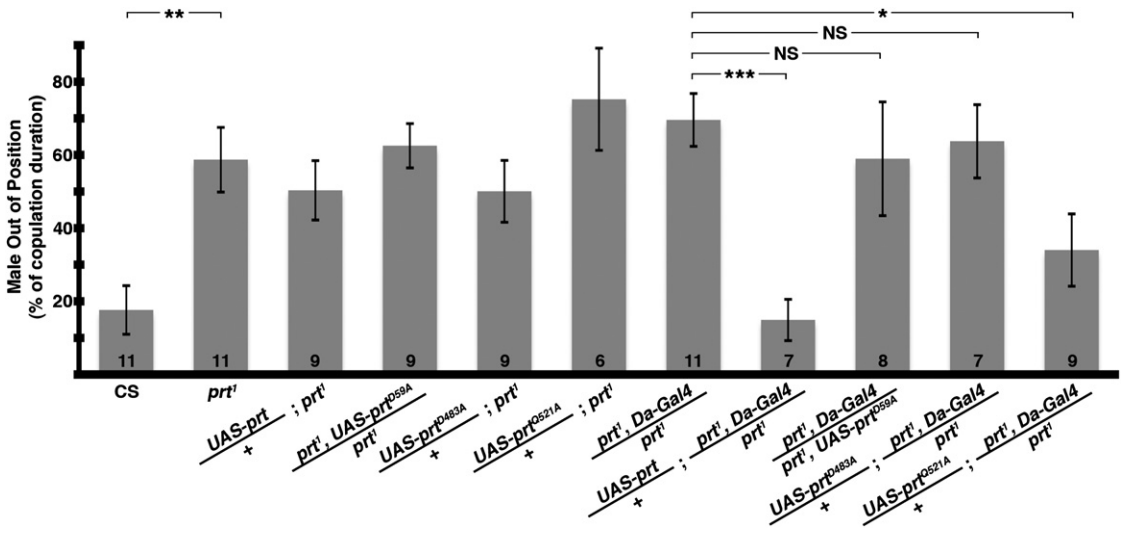

Figure 8. Point Mutants of Conserved Aspartates Fail to Rescue Copulation Defect

Transgenic expression with a ubiquitous driver (*Da-Gal4*) rescued the prt^1 copulation phenotype with wild-type PRT (eighth column, $p < 0.001$), but not with the D59A (ninth column) or D483A (tenth column) mutations. In contrast, transgenic expression of the Q521A mutation did rescue the prt^1 copulation phenotype (final column, $p < 0.05$). The driver or *UAS-prt* transgenes alone did not rescue the behavior (columns 3–7, $p > 0.05$ for all compared to prt^1). *$p < 0.05$, **$p < 0.01$, ***$p < 0.001$, ANOVA with Bonferroni's posttest for multiple comparisons. The data plotted represents mean ± SEM. The n for each group is shown with each column. NS indicates not significant.

PRT (Figure S1). For both rat VMAT2 and VAChT, mutation of the aspartate in TM10 abolishes transport activity, whereas mutation of the aspartate in TM1 of VMAT2, but not VAChT, inhibits transport (Kim et al., 1999; Merickel et al., 1997; Merickel et al., 1995).

We used site-directed mutagenesis to convert these homologous sites to alanine (D59A or D483A) and expressed each in vivo as a *UAS* transgene. Both *UAS-prt*^{D59A} and *UAS-prt*^{D483A} showed robust expression on western blots (data not shown); however, neither rescued the prt^1 phenotype (Figure 8). Thus, residues conserved in VMAT2, DVMAT, and PRT, and required for VMAT2 activity, are also required for PRT function. Furthermore, the aspartate in TM1 required for both prt^1 rescue and VMAT2 transport activity is not required for VAChT activity. These data support the idea that PRT functions as a vesicular transporter more similar to VMATs than VAChT.

To obtain additional insight into the structural requirements for PRT activity, we turned our attention to another, more ambiguous site. Mutation of a conserved aspartate in TM11 of either VMAT2 or VAChT blocks transport activity (Kim et al., 1999; Merickel et al., 1997); however, PRT contains an uncharged glutamine in TM11 (Q521; star, Figure S1B). The presence of a nonconserved glutamine at this site in PRT suggested that it might not be essential for its activity. Indeed, in contrast to PRT mutants D59A and D483A, the Q521A mutant partially rescued the prt^1 mutant phenotype (Figure 8).

Together, our data suggest that PRT likely functions as a vesicular transporter similar to the VMATs. However, PRT did not display appreciable affinity for known substrates such as dopamine or serotonin in in vitro transport assays with DVMAT as a positive control (data not shown). Moreover, PRT localizes to cells that do not express any of the enzymes required for the synthesis of known monoamines (see below). These data, along with the differential structural requirements for activity, support the possibility that PRT recognizes a substrate distinct from either VMATs or VAChT.

DISCUSSION

We have identified a novel gene *prt* that appears structurally similar to vesicular monoamine and acetylcholine transporters. This gene corresponds to predicted gene *CG10251* and localizes to chromosomal region 3R:95A. PRT is expressed in a subset of cells in both larval and adult nervous systems, including the KCs of the MBs. The prt^1 mutant phenotype includes a reduction in learning and an unusual sexual phenotype, characterized primarily by the inability of males to stay in position during copulation. PRT expression in the KCs and other cells that lack known neurotransmitter systems suggests that *prt* represents the first component of a previously unknown neurotransmitter system in insects and perhaps other species.

At present it is difficult to perform biochemical assays to conclusively demonstrate PRT transport activity because we do not know its substrate(s), and we believe that it recognizes a previously unknown neurotransmitter. We have attempted to circumvent this limitation using a genetic approach to test whether sites required for transport in VMAT and VAChT are also required for PRT function in vivo. We focused on two sites conserved in PRT, VMAT, and VAChT: aspartates in TM1 and TM10. Both are required for VMAT transport activity, and the TM10 aspartate is required for transport activity in VAChT. We found that mutation of either site in PRT (D59A and D483A) abrogates its ability to rescue the prt^1 mutant phenotype. Thus, given (1) that PRT is the only member of the vesicular transporter family present in KCs, (2) the likelihood that KCs, like all other neurons,

exocytotically release at least one type of classical or amino acid neurotransmitter, and (3) the fact that two sites required for transport activity in VMAT are also required for the function of PRT in vivo, we propose that PRT functions to store an unknown neurotransmitter in secretory vesicles of at least a subset of KCs, as well as other neurons, and is an "orphan" vesicular transporter.

It is possible that the PRT substrate is a previously identified small molecule. This substrate would presumably be similar to monoamines because PRT is similar to VMAT, and mutation of a site that abolishes transport in VMAT, but not VAChT (D59 in TM1), blocks PRT activity in vivo. However, PRT's primary structure differs from VMAT at several key sites (Figure S1; Parsons, 2000). Most notably, a charged amino acid conserved in VMATs (as well as in VAChT) in TM11 is an uncharged glutamine in PRT. Whereas mutation of the analogous aspartate in VMAT and VAChT completely blocks transport activity, a mutant form of PRT containing an alanine at this site (Q521A) is able to partially rescue the *prt*^{1} mutant behavioral phenotype. We therefore speculate that PRT transports and some KCs employ a compound not previously recognized as a neurotransmitter. Importantly, this would explain why the enzymes required for the synthesis of all known monoamine neurotransmitters (and acetylcholine) are not expressed in the MBs (Bao et al., 2010; Burg et al., 1993; Cole et al., 2005; Gorczyca and Hall, 1987; Konrad and Marsh, 1987; Monastirioti et al., 1996; Neckameyer and White, 1993). It would also explain why the neurotransmitter released from KCs has remained frustratingly obscure for so many years, despite extensive study of the MBs.

How could a novel neurotransmitter remain unknown for so long? First, it may be insect- or invertebrate-specific, and, generally, the neurochemistry of the mammalian brain has received more attention than that of invertebrates. Additionally, subtle phenotypes caused by disrupting this unique neurotransmitter system may have escaped previous genetic screens. Despite the copulation defect, *prt*^{1} mutants are fertile and males court successfully, albeit less avidly. Similarly, the learning phenotype of *prt*^{1} is relatively subtle compared to some other mutants and could easily have been overlooked. More generally, it is important to recall that the identification of most neurotransmitters has lagged far behind the physiological and behavioral characterization of their attendant cells and circuits. Decades elapsed between the characterization of dopamine as a precursor for noradrenaline and the determination that it functions as a bona fide transmitter. We also note that serotonin, histamine, GABA, and glutamate were not fully acknowledged to be neurotransmitters until the 1970s. Although the chemical released from KCs may also be familiar to biologists as an intermediate metabolite, there are multiple precedents for known molecules having eluded identification as neurotransmitters.

The *prt*^{1} Phenotype

We find that *prt*^{1} mutants show behavioral deficits in learning and sexual behavior. Another mutation that influences both the MBs and sexual behavior is the *icebox* allele of *neuroglian*, an L1-type cell adhesion molecule, which results in reduced female receptivity, subtle changes in male courtship, and dramatic structural abnormalities of the MBs (Carhan et al., 2005). In addition, classical olfactory learning mutants, such as *dunce*, *amnesiac*, and *rutabaga*, similarly affect experience-dependent modification of sexual behavior (Ackerman and Siegel, 1986; Gailey et al., 1984).

The localization of PRT to the MBs is consistent with the *prt*^{1} learning phenotype, but given the well-established importance of the MBs for learning, we were initially surprised that *prt*^{1} showed a relatively mild learning deficit. There are several possible explanations for this apparent discrepancy. For example, PRT may reside mainly in subsets of KCs required for MB functions other than learning. Despite the robust MB labeling, it is difficult to say whether PRT expresses in only a fraction of adult KCs. Alternatively, *prt*^{1} mutants may have undergone an adaptive response that minimizes the effects of the mutation on some circuits, such as those required for learning, whereas other PRT circuits may be less able to adapt, such as those required for copulatory behavior.

The *prt*^{1} copulation phenotype is dramatic and unusual. Previously described mutant flies with defects in copulation include the following: *dissatisfaction*, in which males have difficulty curling their abdomens and females are unreceptive during both courtship and copulation (Finley et al., 1997); *celibate* (Hall and Greenspan, 1979), *nerd* (Ferveur and Jallon, 1993), and *platonic* (Yamamoto et al., 1997), all of which court normally but fail to initiate copulation; and *coitus interuptus* (Hall and Greenspan, 1979) and *okina* (Yamamoto et al., 1997), both of which shorten copulation. In addition, certain combinations of *fruitless* alleles lengthen copulation (Lee et al., 2001), and *lingerer* (Kuniyoshi et al., 2002) mutants cannot terminate copulation.

None of these previously described mutants phenocopy the positioning defect of *prt*^{1}. Rather, the most similar deficit reported is in flies in which selected sensilla have been manually removed (Acebes et al., 2003). Male flies use mechanosensory sensilla on their claspers and lateral plates for proprioception during copulation, and ablation of these sensilla results in asymmetrical mating postures. Although the terminalia of *prt*^{1} males are indistinguishable from wild-type, it remains possible that other peripheral deficits contribute to the observed defect in copulation. However, our data thus far suggest that the *prt*^{1} behavioral phenotype is due to deficits in the function of the nervous system, because expression of PRT in the MBs using the *OK107-Gal4* driver completely rescues the behavioral phenotype. We speculate that male *prt*^{1} flies may have difficulty in either receiving or processing sensory information during copulation. This proposal is consistent with the previously described role of the MBs as centers of sensory integration (Strausfeld et al., 1998; Wessnitzer and Webb, 2006), in addition to their established importance for learning and memory.

Further study of *prt*^{1} may help determine the mechanism by which neurotransmission in the MBs integrates information required for memory and sexual behavior. Furthermore, if PRT indeed functions as a vesicular transporter, the determination of its substrate will identify the elusive neurotransmitter that is stored in Kenyon cells.

EXPERIMENTAL PROCEDURES

Animals

D. melanogaster strains were obtained from the Bloomington Stock Center. The wild-type Canton-S strain was used for all studies except as indicated

in the text. Flies were maintained on standard molasses-agar media at 25°C under a 12 hr light-dark cycle.

cDNA Cloning and Expression Constructs

RT-PCR was performed using head RNA isolated as described (Greer et al., 2005), followed by amplification using the SuperScript One Step RT-PCR System (Invitrogen). We subcloned the predicted coding region of *CG10251* into the pCRII TOPO, pcDNAI Amp, and pMT vectors (Invitrogen) for in vitro expression, and into pExp-UAS (Exelixis) and pUASTattB (Bischof et al., 2007) for expression in vivo. A fragment of the *CG10251* cDNA representing the predicted carboxyl terminus was subcloned into the pGEX KG vector provided by Greg Payne (UCLA) for antibody production. See Supplemental Experimental Procedures for further details.

mRNA Analysis

Amplification of stage-specific cDNAs was performed using *Drosophila* RapidScan Panels (OriGene) and probes generated using the primers DVX1 and DVX6 for *CG10251*. The expression of *CG10251* was normalized to *RP49* by arbitrarily defining the pixel intensity of the *RP49* band in lane 9 as 1.0. The normalized value for *CG10251* for lane n was calculated as the observed pixel intensity for *CG10251* × (*RP49* lane n/*RP49* lane 9). Northern blots were performed as described (Greer et al., 2005) using a probe generated with the primers unk19A2 and unk19B2. See Supplemental Experimental Procedures for primer sequences.

Antibody Production

The glutathione S-transferase fusion protein encoding the C terminus of CG10251 was used by Cocalico Biologicals to generate an antiserum in rabbits. The antiserum was affinity purified using the fusion protein immobilized on nitrocellulose as described previously (Greer et al., 2005).

Protein Expression and Detection

S2 cells were transfected and expression was induced using the metallothionein promoter in pMT vector, and western blots were performed as described previously (Chang et al., 2006; Greer et al., 2005), with the antiserum to CG10251/PRT used at a concentration of 1/1,000. For western blot analysis of glycerol velocity and sucrose density gradients (see below), primary antibodies included mouse anti-HA.11 (1:1,000; Covance Research Products) to detect CG10251/PRT, mouse mAb to detect *Drosophila* cysteine string protein (DCSP; 1:1,000; Developmental Studies Hybridoma Bank; Zinsmaier et al., 1990), rabbit anti-late bloomer (lbm; 1:250), a gift of Aaron DiAntonio (Washington University) as marker for the plasma membrane, and rabbit anti-ANF antibody (1:4,000; Peninsula Laboratories/Bachem) as a marker for LDCVs. Either anti-mouse or anti-rabbit HRP conjugated secondary antibodies were incubated (1:2,000, Amersham Biosciences) for 45 min at ambient temperature, followed by SuperSignal West Pico Luminol/Peroxide (Pierce), and exposure to Kodak Biomax Light Film.

Glycerol Velocity Gradient Fractionation

Flies containing *UAS-prt-HA* driven by a panneuronal driver *elav-Gal4* were used. Glycerol gradient fractionation was performed as described (Daniels et al., 2004).

Sucrose Density Gradient Fractionation

Frozen adult fly heads were homogenized in 10 mM K HEPES, pH 7.4, 1 mM Na EGTA, 0.1 mM $MgCl_2$, proteinase inhibitor cocktail (Roche), and 2 mM dithiothreitol (DTT) and were centrifuged for 1 min at 10,000 × *g*, 4°C to obtain the postnuclear supernatant. After addition of EDTA to 10 mM, the supernatant was loaded onto a 20%–55% linear weight per volume sucrose gradient in 10 mM HEPES, pH 7.4, 1 mM EGTA, 1mM $MgCl_2$, and 2 mM DTT. After centrifugation at 30,000 rpm (~111,000 × *g*) for 12–16 hr, 4°C in a Beckman SW 41 Ti rotor, 15 fractions were collected from the bottom of the tube and analyzed by western blot.

Immunohistochemistry

Wandering third-instar larvae and adult flies were dissected in 4% paraformaldehyde and immunofluorescently labeled as described (Greer et al., 2005), with 1:300 anti-PRT and 1:400 goat anti-rabbit Cy3 (Jackson ImmunoResearch) or 1:1,000 goat anti-rabbit Alexa Fluor 488 (Invitrogen) as secondary antibodies.

P Element Excision

To excise a *SUPor-P* element from the 5′UTR of *prt* in the line KG07780, KG07780 homozygotes were crossed to flies containing the Δ2-3 transposase marked with *Sb* in a *yw* background using standard genetic techniques. The progeny were screened for loss of the y^+ body color phenotype, rather than loss of the w^+ eye color, because *SUPor-P* in KG07780 rescues y^-, but not w^-. To screen for loss of the 5′ end of the P and/or the 5′ end of *prt*, genomic DNA from heterozygotes was amplified using the primers DVX8 and Pele5R, representing the 5′ end of the P. Lines showing a loss of the 850 bp amplicon seen in the parent were rescreened using the primer pair DVXCG4 and DVX8 to detect small deletions and the primer pair DVXCG2 and DVX6 to detect larger deletions. The deletion in DVXΔ50 line was confirmed and further characterized using the 3′ primers DVX4 and DVX6 with the 5′ primers DVXCG1, DVXCG2, and DVXCG3. See Supplemental Experimental Procedures for primer sequences.

Histology and Volumetric Measurement

For gross anatomical visualization, flies were prepared for mass histology as described (Heisenberg and Bohl, 1979) and processed with hematoxylin and eosin staining. For volumetric analysis, cold anesthesia was used, and sections were not stained. Anatomy was imaged under fluorescence microscopy double blind with respect to genotype. MB calyx and CCX volumes were derived from planimetric measurements (de Belle and Heisenberg, 1994). CCX measurements summated volumes for the ellipsoid and fan-shaped bodies.

Fly Husbandry for Behavioral Assays

Flies were housed on standard molasses media at 25°C on a 12 hr light-dark cycle and were passed into fresh tubes both the night before and the morning of behavioral testing. Unless otherwise noted, all fly lines used for behavioral analysis were outcrossed into a CS background for at least six generations to minimize any effects of genetic background on behavior (de Belle and Heisenberg, 1996). Cold anesthesia and gentle aspiration were used to manipulate flies prior to all behavioral experiments. Flies were allowed to recover from anesthesia for a minimum of 48 hr before analysis.

Olfactory Associative Conditioning

Learning and memory experiments were performed as described (de Belle and Heisenberg, 1994). Octanol (10^{-4}) and benzaldehyde (2×10^{-4}) diluted in heavy mineral oil (Sigma) were used as the training odors and 90 V was used for the associated shock. Flies were tested immediately after training to measure learning, 30 min after training for short-term memory, and 6 hr after training for middle-term memory.

Courtship

Individual pairs of males and female virgins (3–7 days posteclosion) were placed in 8 mm (inner diameter) by 4 mm (height) polypropylene chambers via aspiration and digitally recorded for 30 min or until copulation. Assays were performed at 23°C in a dedicated test area maintained at 80% humidity to maximize courtship activity. The recordings were scored for selected male courtship behaviors, including following and wing song. A courtship index was calculated as the total time the male spent actively courting as a percentage of the total observation time (Villella et al., 1997).

Copulation

Virgin males and females were collected over ice and housed in same-sex groups of ten for 2–13 days. One naive male and one naive female were gently aspirated into a small chamber (9 mm diameter, 3 mm height), covered with a glass coverslip, and allowed to copulate. The entire copulation event was recorded and scored later by an observer blind to genotype. A male was considered out of position if his midline, as viewed from above, deviated more than 45° laterally or 90° vertically, relative to the female's midline. The time a male spent out of position was measured and reported as a percentage of the total copulation duration.

Fecundity

CS and prt^1 virgin females and young (<1-day-old) males were collected with cold anesthesia and stored overnight in groups of seven. The following day, individual mating pairs, including a male and a virgin female of the same genotype, were introduced into a vial with gentle aspiration. The parents were kept together for 4 days and then removed. Vials with one or two dead parents were discarded. All progeny eclosing within 20 days of the parents' introduction were counted for each mating pair.

Site-Directed Mutagenesis

The QuikChange II XL Site-Directed Mutagenesis Kit (Agilent) was used to introduce the base pair substitutions encoding the D59A, D483A, and Q521A point mutations in PRT. See Table S1 for the primer sequences. The mutants were subcloned into both the pExp-UAS (Exelixis) and pUASTattB (Bischof et al., 2007) vectors to generate *P* element-based and phiC31 integrase based transgenic fly lines.

Genetic Rescue of Copulation Behavior

UAS-prt transgenes were driven by either *Da-Gal4* or *OK107-Gal4*. For rescue with PRT point mutants, *Da-Gal4* was used with *UAS-prt*^{D483A} and wild-type *UAS-prt* inserted on the second chromosome (BDSC stock #24484) via phiC31 recombination (Bischof et al., 2007), as well as *UAS-prt*^{D59A} on the third and *UAS-prt*^{Q521A} on the second chromosome, generated with standard *P* element-mediated transformation (Spradling and Rubin, 1982).

SUPPLEMENTAL INFORMATION

Supplemental Information includes three figures, one table, two movies, and Supplemental Experimental Procedures and can be found with this article online at doi:10.1016/j.neuron.2011.08.032.

ACKNOWLEDGMENTS

We thank Volker Hartenstein for his critical reading of the manuscript and acknowledge David Patton (deceased) for his important contributions to early phases of this work. We would also like to thank Marianne Cilluffo and colleagues at the UCLA Microscopic Techniques Laboratory for their help with paraffin embedding, sectioning, and mounting of histological samples, Alicia Thompson at the USC Center for Electron Microscopy and Microanalysis for her help in performing scanning electron microscopy, and the anonymous reviewers for their excellent suggestions. This work was funded by the National Institutes of Health (MH01709) and the EJLB and Edward Mallinckrodt, Jr. Foundations (D.E.K.), with support from the Stephan & Shirley Hatos Neuroscience Research Foundation (E.S.B., R.R.-C., A.G.), a National Institute of Neurological Diseases and Stroke training grant (T32NS048004) in Neurobehavioral Genetics (E.S.B.), and an National Science Foundation grant (IBN-0237395, J.S.d.B.).

Accepted: August 31, 2011
Published: October 19, 2011

REFERENCES

Acebes, A., Cobb, M., and Ferveur, J.F. (2003). Species-specific effects of single sensillum ablation on mating position in Drosophila. J. Exp. Biol. *206*, 3095–3100.

Ackerman, S.L., and Siegel, R.W. (1986). Chemically reinforced conditioned courtship in Drosophila: responses of wild-type and the dunce, amnesiac and don giovanni mutants. J. Neurogenet. *3*, 111–123.

Ahuja, A., and Singh, R.S. (2008). Variation and evolution of male sex combs in Drosophila: nature of selection response and theories of genetic variation for sexual traits. Genetics *179*, 503–509.

Baier, A., Wittek, B., and Brembs, B. (2002). Drosophila as a new model organism for the neurobiology of aggression? J. Exp. Biol. *205*, 1233–1240.

Bao, X., Wang, B., Zhang, J., Yan, T., Yang, W., Jiao, F., Liu, J., and Wang, S. (2010). Localization of serotonin/tryptophan-hydroxylase-immunoreactive cells in the brain and suboesophageal ganglion of Drosophila melanogaster. Cell Tissue Res. *340*, 51–59.

Bischof, J., Maeda, R.K., Hediger, M., Karch, F., and Basler, K. (2007). An optimized transgenesis system for Drosophila using germ-line-specific phiC31 integrases. Proc. Natl. Acad. Sci. USA *104*, 3312–3317.

Budnik, V., Wu, C.F., and White, K. (1989). Altered branching of serotonin-containing neurons in Drosophila mutants unable to synthesize serotonin and dopamine. J. Neurosci. *9*, 2866–2877.

Burg, M.G., Sarthy, P.V., Koliantz, G., and Pak, W.L. (1993). Genetic and molecular identification of a Drosophila histidine decarboxylase gene required in photoreceptor transmitter synthesis. EMBO J. *12*, 911–919.

Carhan, A., Allen, F., Armstrong, J.D., Hortsch, M., Goodwin, S.F., and O'Dell, K.M. (2005). Female receptivity phenotype of icebox mutants caused by a mutation in the L1-type cell adhesion molecule neuroglian. Genes Brain Behav. *4*, 449–465.

Chang, H.Y., Grygoruk, A., Brooks, E.S., Ackerson, L.C., Maidment, N.T., Bainton, R.J., and Krantz, D.E. (2006). Overexpression of the Drosophila vesicular monoamine transporter increases motor activity and courtship but decreases the behavioral response to cocaine. Mol. Psychiatry *11*, 99–113.

Chaudhry, F.A., Edwards, R.H., and Fonnum, F. (2008). Vesicular neurotransmitter transporters as targets for endogenous and exogenous toxic substances. Annu. Rev. Pharmacol. Toxicol. *48*, 277–301.

Cole, S.H., Carney, G.E., McClung, C.A., Willard, S.S., Taylor, B.J., and Hirsh, J. (2005). Two functional but noncomplementing Drosophila tyrosine decarboxylase genes: distinct roles for neural tyramine and octopamine in female fertility. J. Biol. Chem. *280*, 14948–14955.

Connolly, J.B., Roberts, I.J., Armstrong, J.D., Kaiser, K., Forte, M., Tully, T., and O'Kane, C.J. (1996). Associative learning disrupted by impaired Gs signaling in Drosophila mushroom bodies. Science *274*, 2104–2107.

Crittenden, J.R., Skoulakis, E.M., Han, K.A., Kalderon, D., and Davis, R.L. (1998). Tripartite mushroom body architecture revealed by antigenic markers. Learn. Mem. *5*, 38–51.

Daniels, R.W., Collins, C.A., Gelfand, M.V., Dant, J., Brooks, E.S., Krantz, D.E., and DiAntonio, A. (2004). Increased expression of the Drosophila vesicular glutamate transporter leads to excess glutamate release and a compensatory decrease in quantal content. J. Neurosci. *24*, 10466–10474.

Daniels, R.W., Gelfand, M.V., Collins, C.A., and DiAntonio, A. (2008). Visualizing glutamatergic cell bodies and synapses in Drosophila larval and adult CNS. J. Comp. Neurol. *508*, 131–152.

Davis, R.L. (2011). Traces of Drosophila memory. Neuron *70*, 8–19.

de Belle, J.S., and Heisenberg, M. (1994). Associative odor learning in Drosophila abolished by chemical ablation of mushroom bodies. Science *263*, 692–695.

de Belle, J.S., and Heisenberg, M. (1996). Expression of Drosophila mushroom body mutations in alternative genetic backgrounds: a case study of the mushroom body miniature gene (mbm). Proc. Natl. Acad. Sci. USA *93*, 9875–9880.

Fei, H., Chow, D.M., Chen, A., Romero-Calderón, R., Ong, W.S., Ackerson, L.C., Maidment, N.T., Simpson, J.H., Frye, M.A., and Krantz, D.E. (2010). Mutation of the Drosophila vesicular GABA transporter disrupts visual figure detection. J. Exp. Biol. *213*, 1717–1730.

Ferveur, J.F., and Jallon, J.M. (1993). Nerd, a locus on chromosome III, affects male reproductive behavior in Drosophila melanogaster. Naturwissenschaften *80*, 474–475.

Finley, K.D., Taylor, B.J., Milstein, M., and McKeown, M. (1997). Dissatisfaction, a gene involved in sex-specific behavior and neural development of Drosophila melanogaster. Proc. Natl. Acad. Sci. USA *94*, 913–918.

Gailey, D.A., Jackson, F.R., and Siegel, R.W. (1984). Conditioning mutations in Drosophila melanogaster affect an experience-dependent behavioral modification in courting males. Genetics *106*, 613–623.

Gorczyca, M.G., and Hall, J.C. (1987). Immunohistochemical localization of choline acetyltransferase during development and in Chats mutants of Drosophila melanogaster. J. Neurosci. *7*, 1361–1369.

Greer, C.L., Grygoruk, A., Patton, D.E., Ley, B., Romero-Calderon, R., Chang, H.Y., Houshyar, R., Bainton, R.J., Diantonio, A., and Krantz, D.E. (2005). A splice variant of the Drosophila vesicular monoamine transporter contains a conserved trafficking domain and functions in the storage of dopamine, serotonin, and octopamine. J. Neurobiol. *64*, 239–258.

Hall, J.C., and Greenspan, R.J. (1979). Genetic Analysis of Drosophila Neurobiology. Annu. Rev. Genet. *13*, 127–195.

Heisenberg, M., and Bohl, K. (1979). Isolation of anatomical brain mutants of *Drosophila* by histological means. Z. Naturforsch. C *34c*, 143–147.

Jagadeeshan, S., and Singh, R.S. (2006). A time-sequence functional analysis of mating behaviour and genital coupling in Drosophila: role of cryptic female choice and male sex-drive in the evolution of male genitalia. J. Evol. Biol. *19*, 1058–1070.

Joiner, W.J., Crocker, A., White, B.H., and Sehgal, A. (2006). Sleep in Drosophila is regulated by adult mushroom bodies. Nature *441*, 757–760.

Keene, A.C., and Waddell, S. (2007). Drosophila olfactory memory: single genes to complex neural circuits. Nat. Rev. Neurosci. *8*, 341–354.

Kim, M.H., Lu, M., Lim, E.J., Chai, Y.G., and Hersh, L.B. (1999). Mutational analysis of aspartate residues in the transmembrane regions and cytoplasmic loops of rat vesicular acetylcholine transporter. J. Biol. Chem. *274*, 673–680.

Kitamoto, T., Wang, W., and Salvaterra, P.M. (1998). Structure and organization of the Drosophila cholinergic locus. J. Biol. Chem. *273*, 2706–2713.

Konrad, K.D., and Marsh, J.L. (1987). Developmental expression and spatial distribution of dopa decarboxylase in Drosophila. Dev. Biol. *122*, 172–185.

Kuniyoshi, H., Baba, K., Ueda, R., Kondo, S., Awano, W., Juni, N., and Yamamoto, D. (2002). lingerer, a Drosophila gene involved in initiation and termination of copulation, encodes a set of novel cytoplasmic proteins. Genetics *162*, 1775–1789.

Lawal, H.O., Chang, H.Y., Terrell, A.N., Brooks, E.S., Pulido, D., Simon, A.F., and Krantz, D.E. (2010). The Drosophila vesicular monoamine transporter reduces pesticide-induced loss of dopaminergic neurons. Neurobiol. Dis. *40*, 102–112.

Lee, G., Villella, A., Taylor, B.J., and Hall, J.C. (2001). New reproductive anomalies in fruitless-mutant Drosophila males: extreme lengthening of mating durations and infertility correlated with defective serotonergic innervation of reproductive organs. J. Neurobiol. *47*, 121–149.

Levitt, P., Harvey, J.A., Friedman, E., Simansky, K., and Murphy, E.H. (1997). New evidence for neurotransmitter influences on brain development. Trends Neurosci. *20*, 269–274.

Liu, G., Seiler, H., Wen, A., Zars, T., Ito, K., Wolf, R., Heisenberg, M., and Liu, L. (2006). Distinct memory traces for two visual features in the Drosophila brain. Nature *439*, 551–556.

Merickel, A., Rosandich, P., Peter, D., and Edwards, R.H. (1995). Identification of residues involved in substrate recognition by a vesicular monoamine transporter. J. Biol. Chem. *270*, 25798–25804.

Merickel, A., Kaback, H.R., and Edwards, R.H. (1997). Charged residues in transmembrane domains II and XI of a vesicular monoamine transporter form a charge pair that promotes high affinity substrate recognition. J. Biol. Chem. *272*, 5403–5408.

Miyaji, T., Echigo, N., Hiasa, M., Senoh, S., Omote, H., and Moriyama, Y. (2008). Identification of a vesicular aspartate transporter. Proc. Natl. Acad. Sci. USA *105*, 11720–11724.

Monastirioti, M. (1999). Biogenic amine systems in the fruit fly Drosophila melanogaster. Microsc. Res. Tech. *45*, 106–121.

Monastirioti, M., Gorczyca, M., Rapus, J., Eckert, M., White, K., and Budnik, V. (1995). Octopamine immunoreactivity in the fruit fly Drosophila melanogaster. J. Comp. Neurol. *356*, 275–287.

Monastirioti, M., Linn, C.E., Jr., and White, K. (1996). Characterization of Drosophila tyramine beta-hydroxylase gene and isolation of mutant flies lacking octopamine. J. Neurosci. *16*, 3900–3911.

Nagaya, Y., Kutsukake, M., Chigusa, S.I., and Komatsu, A. (2002). A trace amine, tyramine, functions as a neuromodulator in Drosophila melanogaster. Neurosci. Lett. *329*, 324–328.

Neckameyer, W.S., and White, K. (1993). Drosophila tyrosine hydroxylase is encoded by the pale locus. J. Neurogenet. *8*, 189–199.

Ng, C.S., and Kopp, A. (2008). Sex combs are important for male mating success in Drosophila melanogaster. Behav. Genet. *38*, 195–201.

Nirenberg, M.J., Liu, Y., Peter, D., Edwards, R.H., and Pickel, V.M. (1995). The vesicular monoamine transporter 2 is present in small synaptic vesicles and preferentially localizes to large dense core vesicles in rat solitary tract nuclei. Proc. Natl. Acad. Sci. USA *92*, 8773–8777.

Noveen, A., Daniel, A., and Hartenstein, V. (2000). Early development of the Drosophila mushroom body: the roles of eyeless and dachshund. Development *127*, 3475–3488.

O'Dell, K.M., Armstrong, J.D., Yang, M.Y., and Kaiser, K. (1995). Functional dissection of the Drosophila mushroom bodies by selective feminization of genetically defined subcompartments. Neuron *15*, 55–61.

Parsons, S.M. (2000). Transport mechanisms in acetylcholine and monoamine storage. FASEB J. *14*, 2423–2434.

Popov, A.V., Sitnik, N.A., Savvateeva-Popova, E.V., Wolf, R., and Heisenberg, M. (2003). The role of central parts of the brain in the control of sound production during courtship in Drosophila melanogaster. Neurosci. Behav. Physiol. *33*, 53–65.

Rao, S., Lang, C., Levitan, E.S., and Deitcher, D.L. (2001). Visualization of neuropeptide expression, transport, and exocytosis in Drosophila melanogaster. J. Neurobiol. *49*, 159–172.

Romero-Calderón, R., Shome, R.M., Simon, A.F., Daniels, R.W., DiAntonio, A., and Krantz, D.E. (2007). A screen for neurotransmitter transporters expressed in the visual system of Drosophila melanogaster identifies three novel genes. Dev. Neurobiol. *67*, 550–569.

Sakai, T., and Kitamoto, T. (2006). Differential roles of two major brain structures, mushroom bodies and central complex, for Drosophila male courtship behavior. J. Neurobiol. *66*, 821–834.

Sawada, K., Echigo, N., Juge, N., Miyaji, T., Otsuka, M., Omote, H., Yamamoto, A., and Moriyama, Y. (2008). Identification of a vesicular nucleotide transporter. Proc. Natl. Acad. Sci. USA *105*, 5683–5686.

Schäfer, S., Bicker, G., Ottersen, O.P., and Storm-Mathisen, J. (1988). Taurine-like immunoreactivity in the brain of the honeybee. J. Comp. Neurol. *268*, 60–70.

Schürmann, F.W. (2000). Acetylcholine, GABA, glutamate and NO as putative transmitters indicated by immunocytochemistry in the olfactory mushroom body system of the insect brain. Acta Biol. Hung. *51*, 355–362.

Serway, C.N., Kaufman, R.R., Strauss, R., and de Belle, J.S. (2009). Mushroom bodies enhance initial motor activity in Drosophila. J. Neurogenet. *23*, 173–184.

Sinakevitch, I., Farris, S.M., and Strausfeld, N.J. (2001). Taurine-, aspartate- and glutamate-like immunoreactivity identifies chemically distinct subdivisions of Kenyon cells in the cockroach mushroom body. J. Comp. Neurol. *439*, 352–367.

Spradling, A.C., and Rubin, G.M. (1982). Transposition of cloned P elements into Drosophila germ line chromosomes. Science *218*, 341–347.

Strausfeld, N.J., Hansen, L., Li, Y., Gomez, R.S., and Ito, K. (1998). Evolution, discovery, and interpretations of arthropod mushroom bodies. Learn. Mem. *5*, 11–37.

Strauss, R. (2002). The central complex and the genetic dissection of locomotor behaviour. Curr. Opin. Neurobiol. *12*, 633–638.

Tanaka, N.K., Tanimoto, H., and Ito, K. (2008). Neuronal assemblies of the Drosophila mushroom body. J. Comp. Neurol. *508*, 711–755.

Tokunaga, C. (1961). The differentiation of a secondary sex comb under the influence of the gene engrailed in Drosophila melanogaster. Genetics *46*, 157–176.

Villella, A., Gailey, D.A., Berwald, B., Ohshima, S., Barnes, P.T., and Hall, J.C. (1997). Extended reproductive roles of the fruitless gene in Drosophila melanogaster revealed by behavioral analysis of new fru mutants. Genetics *147*, 1107–1130.

Waddell, S., Armstrong, J.D., Kitamoto, T., Kaiser, K., and Quinn, W.G. (2000). The amnesiac gene product is expressed in two neurons in the Drosophila brain that are critical for memory. Cell *103*, 805–813.

Wessnitzer, J., and Webb, B. (2006). Multimodal sensory integration in insects—towards insect brain control architectures. Bioinspir. Biomim. *1*, 63–75.

Yamamoto, D., Jallon, J.M., and Komatsu, A. (1997). Genetic dissection of sexual behavior in Drosophila melanogaster. Annu. Rev. Entomol. *42*, 551–585.

Yasuyama, K., Meinertzhagen, I.A., and Schürmann, F.W. (2002). Synaptic organization of the mushroom body calyx in Drosophila melanogaster. J. Comp. Neurol. *445*, 211–226.

Zinsmaier, K.E., Hofbauer, A., Heimbeck, G., Pflugfelder, G.O., Buchner, S., and Buchner, E. (1990). A cysteine-string protein is expressed in retina and brain of Drosophila. J. Neurogenet. *7*, 15–29.